

Predicting Structural Permeability in the Deep Coal Play, Tirrawarra-Gooranie fields, Cooper Basin

Bowker, C.J.*
Santos Ltd.
60 Flinders St, Adelaide SA 5000
cameron.bowker@santos.com

Camac, B.A.
Santos Ltd.
60 Flinders St, Adelaide SA 5000
bronwyn.camac@santos.com

Fraser, S.A.
Santos Ltd.
60 Flinders St, Adelaide SA 5000
sam.fraser@santos.com

SUMMARY

A 2D numerical stress modelling study was conducted for the Tirrawarra-Gooranie oil and gas field in the Cooper Basin, which produces from a mixture of conventional and non-conventional (deep coal) reservoirs. The aim of this study is to understand the current state of stress, both magnitudes and orientation, within the zones of interest. A high confidence 3D structural framework was used as a key input to the model, which sought to demonstrate how the in-situ stress is distributed or perturbed throughout the field. The understanding of the current stress state at borehole scale can assist with the prediction of natural fractures or structural permeability, fracture stimulation design and placement, and production performance.

Extensive sensitivity studies were conducted, with the most important inputs found to be boundary stress magnitudes and stress orientation with respect to the faults. The models were interrogated at both the primary coal target and the underlying sandstone horizons. They were found to have significantly different stress states. The output models were compared against production data, 1D mechanical earth models, fracture stimulation data, image logs and core data. The model predictions are in reasonable agreement with the mechanical earth models and the stress orientations determined from the image logs. Predicted stress rotations greater than 4° from the regional stress direction appear to be associated with poorer frac placement, higher bottom hole treating pressures and poor gas rate outcomes. There is a clear association of mineralised natural fractures with areas of low differential stress. The models provide an additional element of subsurface information which will inform future appraisal activities and may improve the understanding of variability in the deep coal fracture stimulation outcomes.

Key words: numerical stress modelling, distinct element method, UDEC, deep coal, Cooper Basin, non-conventional gas, fracture stimulation, Tirrawarra Field

INTRODUCTION

Successful exploration and appraisal of continuous or non-conventional petroleum reservoirs requires an interdisciplinary approach that integrates engineering, geology and geophysics. The production of gas and gas liquids from deep (>2500m) Permian coal seams of the Cooper Basin is an emerging and commercially significant play (Hall *et al.*, 2016; Greenstreet, 2016). The deep coals are the source of the hydrocarbons in the conventional sandstone reservoirs of the Cooper Basin. However, significant volumes of hydrocarbons have been retained within the coal source rock, which is the target of this play. The Permian coals are over-saturated with both free and adsorbed gas and do not require any de-watering to initiate production. They do however require comparatively large conductive fracture stimulations (150 klb to 250 klb of proppant per stage), for economic flow rates to be achieved. Sustained gas production from the deep coal reservoirs has been demonstrated from a growing number of fracture stimulation trials in development wells with commingled production from conventional and non-conventional zones. This data set is now large enough to begin investigating potential influences on single-zone fracture stimulation performance.

Previous studies on fracture stimulation performance in the Cooper Basin have focussed on either conventional sandstone reservoirs (Nelson *et al.*, 2007) or tight sands and shales (Scott *et al.*, 2013). These studies considered the geological, geomechanical and fracture stimulation data at individual well locations. They found that relationships exist between elastic rock properties, geological weaknesses (natural fractures), in-situ stress and stimulation treating pressures. High treating pressures are thought to be associated with high fracture complexity, with higher probability of screen-out leading to poor economic outcomes in those reservoir lithologies. There remains significant uncertainty as to the interplay between fracture stimulation design, in-situ stress, elastic rock properties, natural fractures and production performance in the deep coal. Data analysis from appraisal activities is critical for reducing uncertainty in the distribution of rate and reserve outcomes. It also allows for trends between the multitude of engineering and geological variables to be analysed.

Whilst fracture stimulation parameters are routinely measured and recorded at surface, estimating the local in-situ stress state in the form of a 1D mechanical earth model (MEM) requires specific log suites, calibrated to rock strength data, which are not always available for every well and formation. Further, it has been shown that in-situ stresses can vary greatly within small distances, due to local perturbations of the stress field around discontinuities such as faults (Camac *et al.*, 2006). Therefore, linear interpolation of stress tensor components between wells with 1D MEMs can be misleading, and does not necessarily allow field-scale stress tensor variations and rotations to be understood at locations offset from control wells.

It is possible to model stress perturbations in discontinuous media using the Distinct Element Method (DEM), first introduced by Cundall (1971). This numerical method was developed into the Universal Distinct Element Code (UDEC), and has been used extensively in mining, geotechnics, civil engineering and tectonics for modelling 2D rock stress and stability problems in faulted or fractured media. UDEC has also been used in petroleum exploration for risking of cap-seal failure at the play and prospect levels, by helping to understand the distribution of natural fractures associated with high differential stress (Camac *et al.*, 2009). It has been shown that such models are highly sensitive to the position and orientation of the faults with respect to the regional stress field (Hunt *et al.*, 2003). Therefore, it is critical that rigorous structural interpretation is completed in 3D, and the tectonic history understood for the area of interest prior to numerical stress model initialisation.

This study focussed on the Tirrawarra-Gooranie oil and gas field complex in the South Australian portion of the Cooper Basin. The field complex is the most highly appraised area for the Permian deep coal resource, with over 12 fracture stimulation trials to date, each with at least one production log confirming gas production contributions from coal. The area also has a large amount of data from decades of conventional exploitation including 3D seismic; >100 well intersections with a variety of log-suites; >25 full-hole cores; and a rich set of fracture stimulation and geomechanical data. A detailed 3D structural framework model was completed for the field in 2016, which integrated the local 3D seismic and regional knowledge of the structural evolution of the Cooper Basin (Apak, 1994; Apak *et al.*, 1997; Gravestock *et al.*, 1998). This robust structural framework ensured that the best possible UDEC stress model could be constructed. The model was subjected to an extensive sensitivity study with multiple iterations, before final 'base cases' were created for both the Patchawarra VC40/50 coal and the underlying sandstone horizons. These models have been compared against other field data such as production rates, single well 1D MEMs, fracture stimulation data, image logs and core, to investigate the interplay between in-situ stress and other factors affecting deep coal fracture stimulation performance.

GEOLOGY OF THE TIRRAWARRA-GOORANIE COMPLEX

The Permian to Triassic age Cooper Basin is a mildly compressional structural depression eroded at basin flanks, and is unconformably overlain by the Jurassic to Early Cretaceous Eromanga Basin (Apak, *et al.*, 1997). Coals and fluvio-lacustrine clastic sediments of the Cooper Basin were deposited during and following a deglaciation period with phases of mild tectonic compression. The Cooper Basin is dominated by mild to major inversion structures originating from the unconformably underlying Cambrian to Early Ordovician age Warburton Basin, which is typically considered economic basement in the region (Apak, *et al.*, 1997; Sun, 1999). The 3D structural framework interpretation of the Tirrawarra-Gooranie area completed in 2016 (Figure 1) revealed that the reactivation of these Warburton Basin extensional faults, originally formed during a phase of SE-NW rifting, are key to the evolution of the Permian strata in the Tirrawarra-Gooranie Field complex. The study area is bound to the north and south by large (10-20 km length) east-northeast striking inversion structure trends. Within the Tirrawarra Field, a series of smaller (1-3 km length) north-northeast striking inverted extensional faults and associated antithetic faults propagate steeply up into the Permian section which govern the structural highs of the field. Fault geometries resemble a mildly inverted oblique rift transfer between the larger east-northeast trending fault systems to the north and south of Tirrawarra (Amilibia *et al.*, 2005). A prominent N-S trending left-lateral strike-slip fault cutting through the Tirrawarra field links up the conveniently oriented north-south striking reactivated extensional faults of the Warburton Basin, with repeated Riedel shear faults accommodating a significant proportion of strike-slip strain confined only to the Permian section. The Riedel shears are consistent with an approximately SE-NW maximum horizontal stress (S_{Hmax}) orientation (Wilcox *et al.*, 1973). Mild transpressional step-over structures are developed at relays between fault trends, however a significant amount of deformation is taken up in the major inversion structure to the south of Tirrawarra: hence the mild inversion observed in the study area. In addition, the larger fault systems bounding the Tirrawarra Field are aligned in the preferred orientation for inversion by the estimated paleo S_{Hmax} determined by the Riedel shears, and present day S_{Hmax} (S_{Hmax} orientation approximately E-W to SE-NW).

METHOD AND RESULTS

General UDEC Model Architecture

Unlike the Finite Element Method (FEM), in which the area of interest is modelled with a continuous grid of cells, the Distinct Element Method (DEM) in UDEC handles faults or discontinuities by representing the rock mass as an assembly of discrete 'blocks', the boundaries of which represent the discontinuities (Cundall, 1980). The contact forces and displacements at the boundaries are found through a series of calculations that trace the movement of blocks. All boundaries must completely traverse from one side of a block to another: otherwise they will not be recognised by the program. In practice, true faults do not always connect with other faults, and so-called 'fictitious faults' are required to connect each real fault trace to either an adjacent fault trace or the model area boundary. The 'fictitious fault' properties ensure they have zero slip during the solution cycle, effectively rendering them invisible to the model. The true faults slip and interact with each other according to Coulomb slip theory.

Each fault block is discretised into 'zones', in which the stress, velocity and acceleration are assumed to be constant at each time-step. The greater the number of zones, the finer the resolution and the longer the model takes to run. A time-stepping algorithm is used in which calculations performed alternate between the force-displacement law at all contacts and Newton's second law at all blocks. Calculation continues until all forces are balanced to within a specified tolerance. Detailed stress, strain, displacement, velocity, acceleration and force information for each zone can then be exported and mapped.

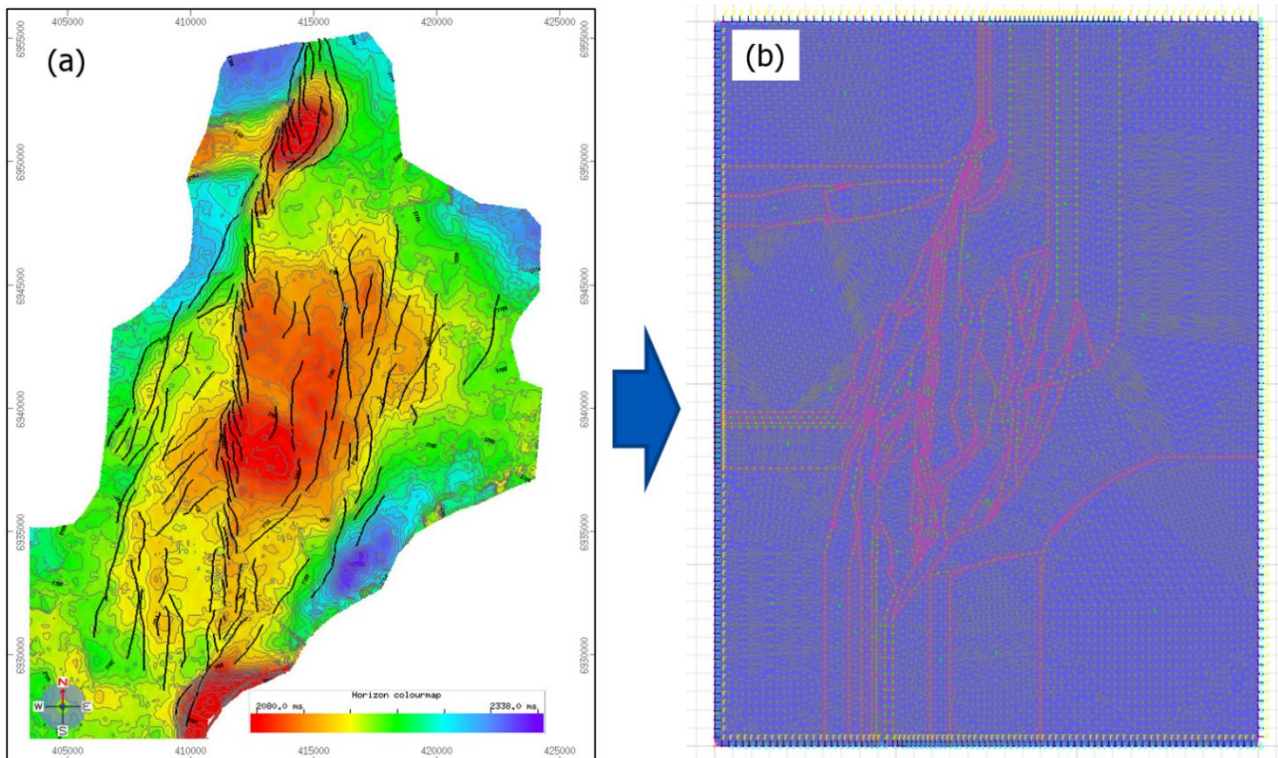


Figure 1: (a) Tirrawarra-Gooranie field 3D structural interpretation. Time-slice at the VC40/50 deep coal horizon level. Colour bar represents seismic two-way travel time, black lines represent fault traces at the VC40/50 horizon. Area is characterised by a north-south trending Riedel shear zone through the centre of the field, with north to north-northeast striking inverted extensional faults and associated antithetic faults on either side of this zone. (b) UDEC 2D representation. Faults have been coarsened, and connected to each other using ‘fictitious faults’ to form discrete blocks. Each block has been discretised into triangular zones, prior to running the time-stepping algorithm.

Transferring Fault Framework from the Tirrawarra-Gooranie Structural Interpretation

The fault polygons at the Patchawarra VC40/50 horizon (Figure 1(a)) were exported from the 3D structural model, coarsened (i.e. reduced in resolution), and directly imported into the UDEC model. I conducted this coarsening such that a reasonable balance between runtime and model resolution could be achieved.

Figure 1(b) shows the UDEC representation of the structural framework, including the ‘fictitious faults’. I included major bounding faults in the NW and SE of the UDEC model which were located outside the Tirrawarra 3D seismic area used to create the structural model, as they have been shown to have had a major influence on the structural evolution of the field (Apak *et al.*, 1997). I left a wide 5km border between the model area boundary and the faulted area of interest, to prevent any artificial boundary effects skewing the modelled stress perturbations around the true faults.

Model Initialisation

‘Case 1’ was planned as a first-pass model with which I could perform sensitivity checks to understand which parameters had the strongest impact on the model output. Table 1 shows the initial values I used as input parameters for Case 1. I draw particular attention to the boundary stress magnitudes: maximum horizontal stress (S_{Hmax}) and minimum horizontal stress (S_{Hmin}). These inputs I selected from the ranges for regional stress magnitudes given in Reynolds *et al.* (2006). The possible ranges for S_{Hmax} and S_{Hmin} at the regional level were very large, hence I had low confidence in the estimates used in Case 1 as they were arbitrarily selected from within these ranges, and not anchored to any local field-specific data. I later refined the values of the boundary stresses after the sensitivity analysis was completed.

Sensitivity Study

I then conducted an extensive sensitivity study, systematically changing variables to test their effect on the final model output. I did this through visual inspection of the output stress maps, and broadly categorised variables based on their effect as either ‘negligible’, ‘some sensitivity’ or ‘strong sensitivity’. I tested all parameters in Table 1, in addition to other model parameters such as fault stiffness, cohesion, friction angle etc. which had no real-world analogues or corresponding field data, and therefore had to be chosen arbitrarily.

The majority of variables have either negligible or weak effects on the model output. Some of these, such as rock elastic properties or S_v , do have a noticeable effect but only when the input is changed to unrealistically high or low values. The parameters which have the strongest effect include the boundary stress magnitudes, boundary stress orientation and position of the faults. Figure 2 shows the model sensitivity to the orientation of S_{Hmax} at the boundary.

Table 1: Input parameters input for ‘Case 1’ with comments on justification. Case 1 was used as the initial case for sensitivity analysis.

Parameter	Case 1 Value	Comment
Coal Density	1350 kg/m ³	From coal side-wall core triaxial testing
Coal Bulk Modulus	7967 MPa	From coal side-wall core triaxial testing
Coal Shear Modulus	1707 MPa	From coal side-wall core triaxial testing
Boundary S_{Hmax} azimuth	105°N	Average of S_{Hmax} direction estimates for Tirrawarra-Gooranie area, from breakouts and DITFs in image logs.
Boundary S_{Hmax}	116.7 MPa	Upper bound of S_{Hmax} estimates*
Boundary S_{Hmin}	44.2 MPa	Lower bound of S_{Hmin} estimates*
Boundary stress anisotropy ($S_{Hmax} - S_{Hmin}$)	72.5 MPa	Difference between horizontal principal stress magnitudes
Boundary S_v	60.2 MPa	Intermediate estimate*
Boundary velocity	0 m/s	Set to zero to prevent model blocks collapsing/expanding
Pore pressure	28.3 MPa	Hydrostatic for reference depth 2850mTVD
Constitutive Model	Elastic (linear, isotropic)	Simplest model with shortest runtime

*Stress magnitude estimates refer to ranges for the regional Cooper Basin stresses given in Reynolds et al. (2006) at a reference depth of 2850mTVD.

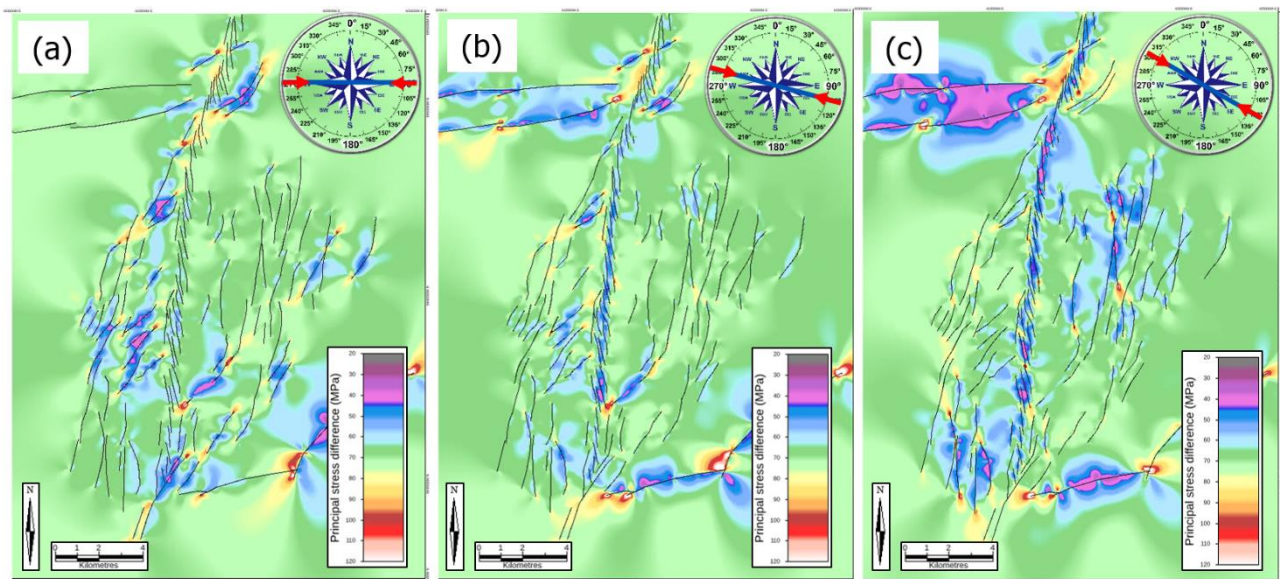


Figure 2: Sensitivity study output for boundary stress orientation investigation. The orientation of the maximum horizontal principal stress (denoted by S_{Hmax} azimuth) is indicated by the arrows on the compass rose in the top right corner of each map. (a) Principal stress difference map for S_{Hmax} azimuth = 90°N (b) Principal stress difference map for ‘Case 1’: S_{Hmax} azimuth = 105°N (c) Principal stress difference map for S_{Hmax} azimuth = 120°N.

Model calibration and final ‘base cases’

I then looked more closely at the local stress magnitudes estimated from the single well 1D Mechanical Earth Models (MEMs), constructed for seven wells within the model area over the Patchawarra Formation. 1D MEMs are estimates of the ‘mechanical stratigraphy’, or the vertical profile of the principal stresses S_v , S_{Hmin} and S_{Hmax} with depth at the wellbore location. They are constructed using equations from frictional faulting theory, with key inputs being sonic and density log suites, and are calibrated to rock strength and in-situ pressure data.

The example in Figure 3 shows how the mechanical stratigraphy can be highly heterogeneous (even within a single formation), reflecting the different stress states in the different lithologies that arise from contrasts in elastic moduli and rock strength. The contrasts can be so extreme that the stress regime can change between normal and strike-slip regime for coals and sandstones, respectively.

It was possible to extract median values of the S_{Hmax} and S_{Hmin} distributions for both coals and non-coals within the Patchawarra Formation from each of the 1D MEMs. These are shown in Table 2. It is apparent that the boundary stress anisotropy used in ‘Case 1’

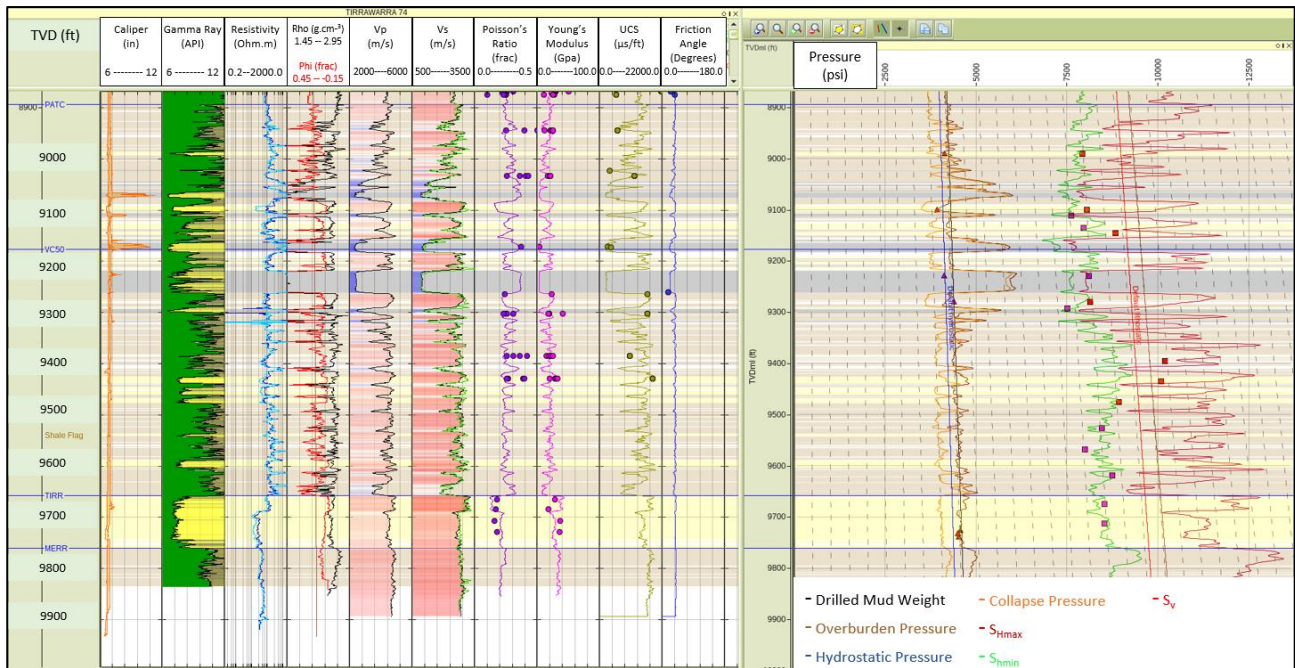


Figure 3: Example 1D Mechanical Earth Model (MEM) for Tirrawarra 74. S_{hmin} , S_v and S_{Hmax} are represented by the green, red and maroon tracks, respectively, in the far right window. This illustrates the highly heterogeneous mechanical stratigraphy, with the stress regime switching between normal and strike-slip conditions for coals (highlighted in grey) and sandstones (highlighted in yellow), respectively.

Table 2: Extracted median S_{hmin} , S_{Hmax} , and principal stress difference values from pre-existing 1D MEMs in the Tirrawarra-Gooranie field. Values were extracted for both the clastic and coal lithologies.

Well	1D MEM median values: Patchawarra clastics (density>1.8g/cc)			1D MEM median values: Patchawarra coals (density<1.8g/cc)		
	S_{hmin} (MPa)	S_{Hmax} (MPa)	Principal Stress Difference (MPa)	S_{hmin} (MPa)	S_{Hmax} (MPa)	Principal Stress Difference (MPa)
Gooranie 1	53.7	77.5	23.8	55.9	59.7	3.8
Gooranie 5	56.5	74.3	17.8	51.8	54.2	2.4
Gooranie 7	53.1	72.9	19.8	49.8	54.1	4.3
Tirrawarra 73	54.2	71.9	17.7	51.8	52.8	1.0
Tirrawarra 75	55.2	73.4	18.2	53.6	55.9	2.3
Tirrawarra 84	51.1	76.0	24.9	48.8	49.8	1.0
Tirrawarra 87	57.0	73.1	16.1	51.5	53.5	2.0
Average	54.0	74.3	20.3	51.9	54.3	2.4

of 72.5MPa is too large for the area, given the average principal stress differences in Table 2. I also observed that the stress anisotropy in the coals is an order of magnitude lower than that for the clastics. Therefore, I proceeded to construct two final 'base cases': one for the coal lithology using the average of the coal stresses from the MEMs as the boundary condition with coal elastic properties; and one for the underlying sandstone lithology using the average clastic stresses from the MEMs with sandstone rock elastic properties.

For each of the final 'base case' models, I interrogated the resultant outputs and extracted stress tensor information at every well location, including S_{hmin} , S_{Hmax} , Mean Stress, S_{Hmax} Azimuth and Principal Stress Difference. Figure 4 shows Principal Stress Difference maps for the sandstone and coal horizons, respectively, as examples. I then compared the stress tensor information against a variety of other field data, for the dual purposes of ground-truthing the model and investigating whether any relationships exist between the predicted in-situ stress and other variables relating to coal production performance.

Comparison of UDEC stress predictions with 1D MEMs

Figure 5 shows a graphical comparison of the UDEC and 1D MEM principal stress difference predictions for the sandstone and coal horizons, respectively. The sandstone model has a reasonable trend, suggesting that the relative stress variations predicted by UDEC are in reasonable agreement with the log data at various well locations. Some scatter is apparent, which can be attributed to the inherent errors in the model, as well as that introduced by representing a heterogeneous vertical stress profile with a single median value. Conversely, there is no apparent trend between the UDEC predictions and the 1D MEMs for the coal horizon stresses, which I attribute to the fact that the relative stress variations are much smaller in magnitude within the coal (which has a nearly isotropic stress regime), whilst the errors in the model are essentially the same for the coal and the sandstone horizons.

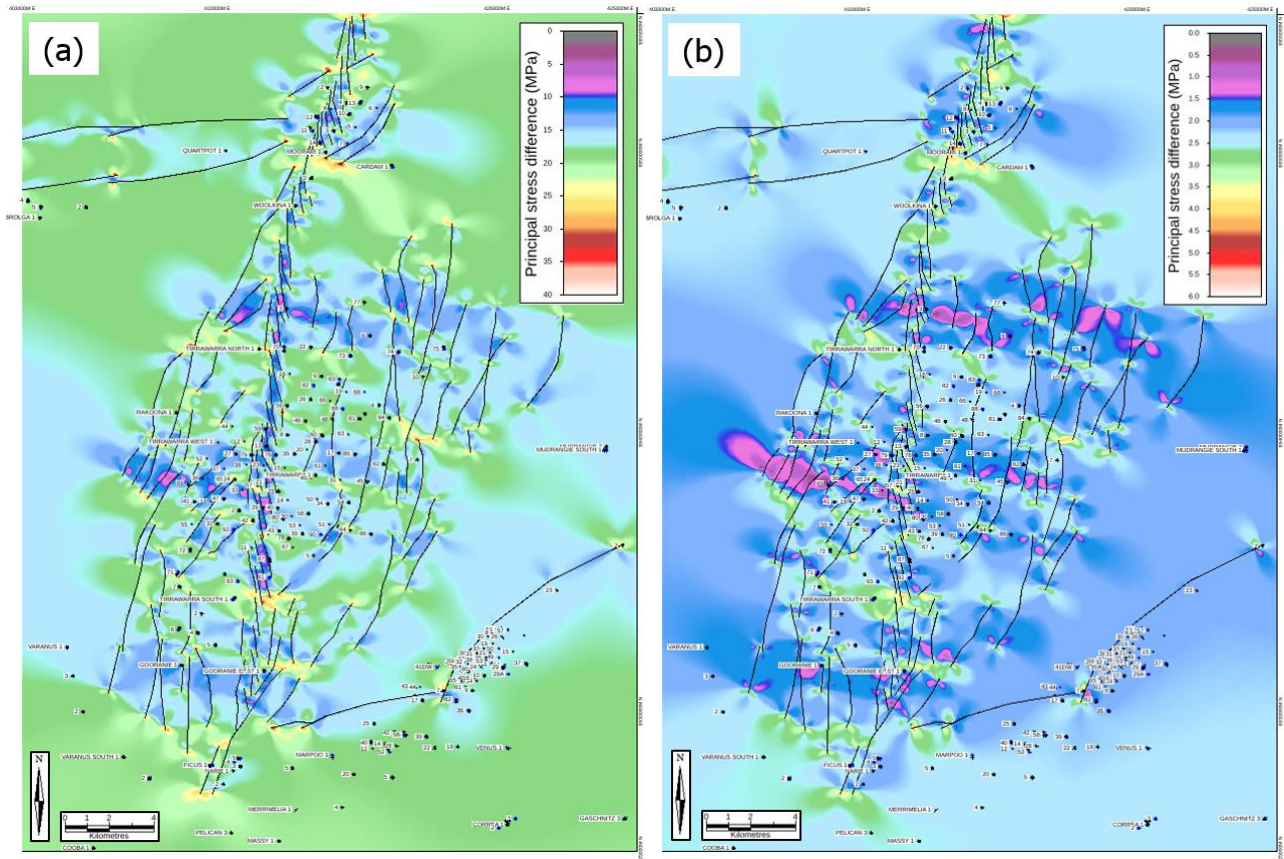


Figure 4: Example final base case output maps, with well locations shown. (a) Sandstone principal stress difference. (b) Coal principal stress difference. Note the different colour bar scales. Stress perturbations generally have similar geometry in the coal and sandstone horizons, however the magnitude of the perturbations are much larger in the sandstones than in the coal.

Comparison of UDEC stress predictions with coal gas rate measurements

I compared the model stress tensor data against 18 coal fracture stimulation trials in the modelling area. I considered all stress tensor components including S_{hmin} , S_{hmax} , Mean Stress and Principal Stress Difference. I could find no clear relationships between coal gas rate and in-situ stress magnitude. In contrast, there does appear to be a trend against stimulation design parameters such as total frac size. This suggests that stimulation design has a stronger influence on the initial gas rate outcome than the in-situ stress magnitude.

Whilst it was difficult to find any relationship between gas rate and stress magnitude, stress *direction* appears to have some influence on the gas rate. Severe rotations of the stress field due to perturbations about faults appear to have a negative influence on frac outcomes. Figure 6 shows coal gas rate (normalised to coal thickness) versus the rotation in the local stress field from the boundary condition. The best gas rate was associated with an area that had nearly no predicted stress rotation, whereas areas with significant rotations (over 4° from the regional) all performed poorly or were technical failures. I also observed that large stress field rotations were associated with higher average bottom hole treating pressures during the fracture stimulation. This seems to imply that local stress field rotations associated with faults may make fracture stimulation more difficult due to higher fracture complexity, which negatively impacts the gas rate performance.

Comparison of UDEC stress predictions to fracture stimulation data

Typically, fracture closure pressures (P_c) from diagnostic fracture injection tests (DFITs) are used as a measure of the local in-situ S_{hmin} magnitude (Zoback, 2007). However, there was not enough of this data available to validate the UDEC model predictions of S_{hmin} variations across the field. Pressure data from the main fracture stimulation operations, such as breakdown pressure and average bottom hole treating pressures (BHTP), was available in quantities large enough for analysis. Using these measurements is expected to be a more error prone way of estimating the in-situ stress, as they depend on other variables such as fluid frictional losses.

For the coal horizon, I observed a low confidence trend between S_{hmin} predictions and frac breakdown pressure. There was a reasonable trend between stress field rotation and average coal frac BHTP, giving me further confidence that predicted stress field rotations are associated with more complex fracture stimulation and hence make placing to design and achieving a good gas rate more difficult. For the sandstone horizon, I observed a reasonable trend between S_{hmin} predictions and frac breakdown pressure, whilst a low confidence trend was apparent between stress field rotation and average sandstone frac BHTP. This could be reflective of the fact that for sandstones, many other variables affect the BHTP such as frictional losses, formation permeability and depletion.

Comparison of UDEC stress predictions with Image Log and Core fracture data

Two interpreted image logs are available for the model area, Tirrawarra 73 and 75. The overall S_{hmax} azimuth was estimated from borehole breakouts and drilling induced tensile failures (DITFs) for both of these image logs, and was approximately 105° which was

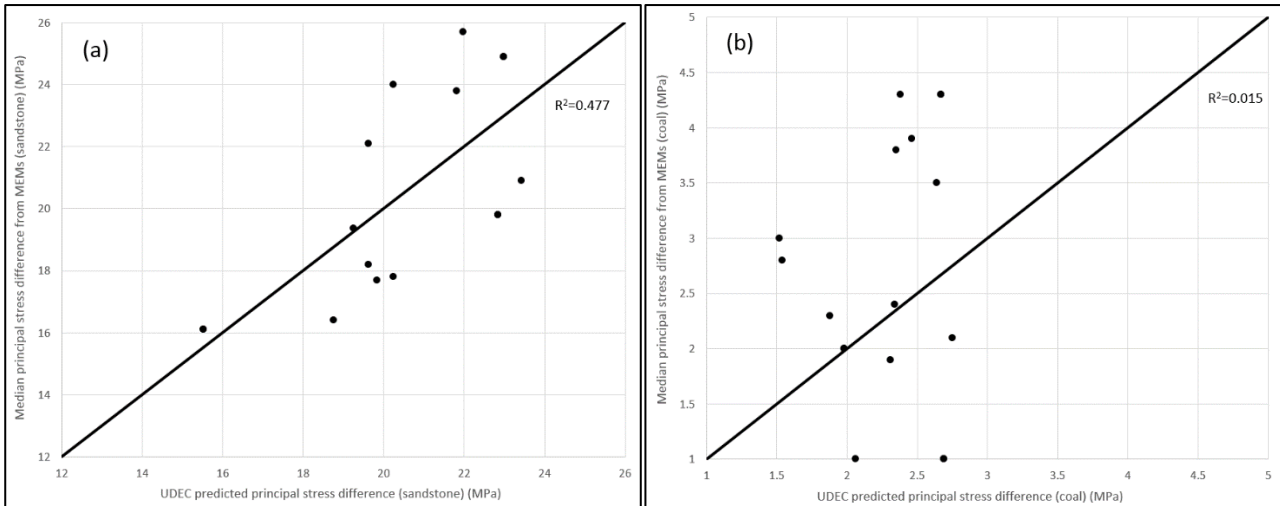


Figure 5: UDEC principal stress predictions versus median principal stress difference calculated from 1D MEMs at 14 well locations. (a) Sandstone horizon. Reasonable trend about the line $x=y$; (b) Coal horizon. No trend.

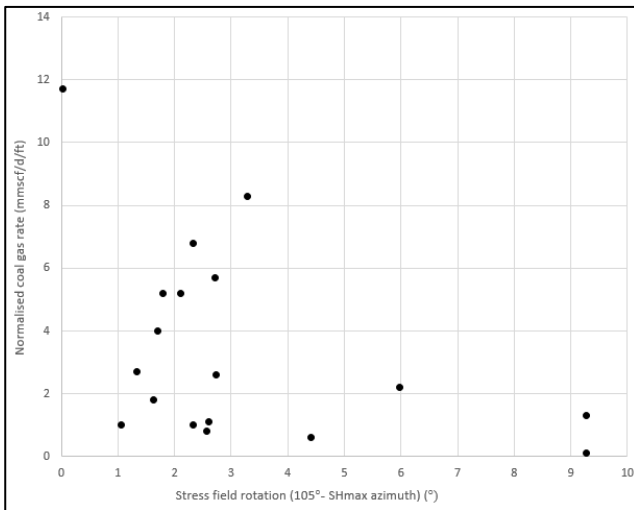


Figure 6: Normalised coal gas rate versus stress field rotation (measured as the absolute value of the difference between the UDEC modelled S_{Hmax} azimuth at the well location and the boundary stress condition $105^\circ N.$) Severe stress field rotations ($>4^\circ$) appear to be associated with poorer frac outcomes and technical failures.

in agreement with the UDEC model predictions for those well locations. Neither of the image logs had any fractures interpreted over the coal, and only Tirrawarra 73 had any fractures interpreted in the entire Patchawarra Formation. Hence it was not possible to use the image logs to see whether the stress model output had any correlation with fracture density in the Patchawarra coals or sandstones.

29 full hole cores had been obtained from the Tirrawarra Field which have been logged. Both ‘open’ and ‘healed’ (or mineralised) fractures were recorded during logging. There were no mineralised fractures in the coals, and there was no way to discern between an open tectonic fracture and core damage in the coal lithology. Therefore, I only used the sandstone UDEC model for comparison with the fracture density data, as the fracture counts were only representative of observations in sandstones. There was a clear association of healed fractures with the Riedel shear zone, an area modelled as having low differential stress. There were no clear patterns or relationships between the structure, in-situ stress state and the open fracture density. When adding the healed and open fracture counts together to give a total fracture density, there appeared to be a trend where areas with higher S_{hmin} and higher mean stress appeared to have greater total fracture density.

CONCLUSIONS

UDEC was used to create 2D numerical stress models for the Tirrawarra-Gooranie oil and gas field complex, for the unconventional deep coal and adjacent sandstone horizon, respectively. This required a rigorous 3D structural geological model to first be built using 3D seismic data. Extensive sensitivity studies were undertaken, to understand the impact of model inputs on the final output. The numerical stress models give insight as to the local stress tensor variations that result from the interaction of the regional current day stress field and field-scale discontinuities such as faults. This is an additional layer of subsurface information that will help to inform future appraisal activities and assist with understanding the variability in fracture stimulation and production outcomes.

The models were compared against various other field data, with the following qualitative observations:

1. Areas with stress field rotations greater than 4° from the regional appeared to have an association with poorer proppant placement during the coal fracs, higher bottom hole treating pressures, and poorer production outcomes.
2. There was good agreement between the sandstone UDEC model and the stress variations seen in the 1D mechanical earth models. In contrast, the coal UDEC model was highly isotropic, therefore the stress variations predicted by the model were too small in magnitude (compared to the errors) to clearly correlate with the variations seen in the 1D mechanical earth models.
3. There was reasonable agreement between the model S_{hmin} predictions and frac breakdown pressures in the sandstone horizon. In contrast, there was very little correlation between the coal horizon S_{hmin} predictions and frac breakdown pressures. Not enough closure pressure data from DFITs existed to see if there was any correlation.
4. The stress orientations estimated from breakouts and DITFs in the two available image logs were in agreement with the model predictions for those locations. No information about fracture density variations in the Patchawarra Formation could be discerned from the image logs.
5. Fracture density data from core logging was compared against the stress models. The only reliable fracture information was for the sandstones. It was not possible to distinguish between fractures and core damage in the coal lithology. There was a clear association of 'healed' or mineralised fractures with the Riedel shear zone, a region with low differential stress predicted by the model. The 'open' fracture density did not have any clear association with any structural features or in-situ stress anomalies.

ACKNOWLEDGMENTS

The authors would like to acknowledge David Wines of Itasca Australia Pty Ltd. for his ongoing advice and technical support during the modelling project. Emma Tavener and her team for support with the generation and understanding of the 1D MEMs used in this study; and also our joint venture partners, Origin Energy and Delhi Petroleum for allowing the publication of this study.

REFERENCES

- Amilibia, A., McClay, K.R., Sabat, F., Munoz, J.A., Roca, E., 2005, Analogue Modelling of Inverted Oblique Rift Systems: *Geologica Acta*, 3(3), 251-271
- Apak, S.N., 1994, Structural development and control on stratigraphy and sedimentation in the Cooper Basin, Northeastern South Australia and Southwestern Queensland, PhD Thesis, University of Adelaide
- Apak, S.N., Stuart, W.J., Lemon, N.M., Wood, G., 1997, Structural Evolution of the Permian-Triassic Cooper Basin, Australia: Relation to Hydrocarbon Trap Styles: *AAPG Bulletin*, 81(4), 533-555
- Camac, B.A., Hunt, S.P., Boulton, P.J., 2006, Local rotations in borehole breakouts – observed and modelled stress field rotations and their implications for the Petroleum Industry: *International Journal of Geomechanics*, 6(6), 399-410
- Camac, B.A., Hunt, S.P., Boulton, P.J., 2009, Predicting brittle cap-seal failure of petroleum traps: an application of 2D and 3D distinct element method: *Petroleum Geoscience*, 15, 75-89
- Cundall, P.A., 1971, A computer model for simulating progressive large scale movements in blocky rock systems: *Proceedings, Symposium of the International Society of Rock Mechanics, Nancy, France, 1, Paper No. II-8*
- Cundall, P.A., 1980, UDEC: A Generalized Distinct Element Program for Modelling Jointed Rock. Report PCAR-I-80, Peter Cundall Associates Report, European Research Office, US Army, Contract, DAJA37-79-C-0548
- Gravestock, D.I., Hibbert, J.E., Drexel, J.F., 1998, The petroleum geology of South Australia 1st edition, Volume 4: Cooper Basin, South Australia Department of Primary Industries and Resources. Report Book, 98/9
- Greenstreet, C., 2015, From play to production: the Cooper unconventional story - 20 years in the making: *The APPEA Journal*, 55(2), 407-407
- Hall, L.S., Palu, T.J., Murray, A.P., Boreham, C.J., Edwards, D.S., Hill, A.J. and Troup, A., 2016, Cooper Basin Petroleum Systems Analysis: Regional Hydrocarbon Prospectivity of the Cooper Basin: Part 3. Record 2016/29. Geoscience Australia, Canberra. <http://dx.doi.org/10.11636/Record.2016.029>

- Hunt, S.P., Camac, B.A., Boulton, P.J., 2003, A parametric analysis and applications of the discrete element method for stress modelling: The 9th Australian New Zealand Conference on Geomechanics
- Nelson, E.J., Chipperfield, S.T., Hillis, R.R., Gilbert, J., McGowen, J., 2007, Using geological information to optimize fracture stimulation practices in the Cooper Basin, Australia: *Petroleum Geoscience*, 13, 3-16.
- Reynolds, S.D., Mildren, S.D., Hillis, R.R., Meyer, J.J., 2006, Constraining stress magnitudes using petroleum exploration data in the Cooper-Eromanga Basins, Australia: *Tectonophysics* 415, 123-140
- Scott, M.P., Stevens, T., Durant, R.H., McGowen, J.M., Thom, W.W., Woodroof, R.A., 2013, Investigating Hydraulic Fracturing in Tight Gas Sand and Shale Gas Reservoirs in the Cooper Basin: SPE Unconventional Resources Conference and Exhibition-Asia Pacific, Brisbane, 11-13 November 2013
- Sun, X., 1999, Report Book 99/00014: South Australia Department of Primary Industries and Resources
- Wilcox, R., Harding, T., Seely, D., 1973, Basic wrench tectonics: *American Association of Petroleum Geology Bulletin*, 57(1), 74-96
- Zoback, M.D., 2007, *Reservoir Geomechanics*: Cambridge University Press